Punjab University
Journal of Mathematics (ISSN 1016-2526)
Vol. 51(5)(2019) pp. 27-42

Sixth-Order Stable Implicit Finite Difference Scheme for 2-D Heat Conduction Equation on Uniform Cartesian Grids with Dirichlet Boundaries

Kainat Jahangir[1], Shafiq Ur Rehman[2], Fayyaz Ahmad[3], Anjum Pervaiz[4]

[1,2,4] Department of Mathematics, University of Engineering and Technology, Lahore, Pakistan.
[3] Department de F´ isicai Enginyeria Nuclear, Universitat Politècnica de Catalunya, Eduard Maristany 10, Barcelona 08019, Spain.
[3]Dipartimento di Scienza e Alta Tecnologia, Universita dell'Insubria, Via Valleggio 11, Como 22100, Italy.
[1,2,3,4] Email: kjmath653@gmail.com, srehman@uet.edu.pk, fahmad@uninsubria.it, anjumpervaiz1@hotmail.com

Received: 23 May, 2018 / Accepted: 28 September, 2018 / Published online: 05 March, 2019

Abstract. Constructing higher-order difference schemes are always challenging for boundary value problems. The core part is to define boundary enclosure in such a way that guarantees stability and uniform order of accuracy for all nodes. In this work, we develop sixth-order implicit finite difference scheme for 2-D heat conduction equation with Dirichlet boundary conditions. The computed generalized eigenvalues of implicit finite difference matrices have negative real parts that guarantees stability in the case of Crank-Nicolson method. The validity of our developed numerical scheme is clearly reflected by the numerical testing.

AMS (MOS) Subject Classification Codes: 65N06; 35G30; 33F05
Key Words: Implicit finite difference scheme, Dirichlet boundary conditions, Heat conduction problem.

1. Introduction

The 2-D heat conduction equation can be written as

$$\frac{\partial u(x,y,t)}{\partial t} = k\left(\frac{\partial^2 u(x,y,t)}{\partial x^2} + \frac{\partial^2 u(x,y,t)}{\partial y^2}\right) + s(x,y,t), \quad 0 < x < L_x,$$
$$0 < y < L_y, \quad 0 < t \leq t_f, \qquad (1.\ 1\ \text{a})$$
$$u(x,y,0) = f(x,y), \quad 0 \leq x \leq L_x, \quad 0 \leq y \leq L_y, \qquad (1.\ 1\ \text{b})$$

under Dirichlet boundary conditions:

$$\begin{aligned} &u(x,0,t) = g_1(x,t), \quad u(x,L_y,t) = g_3(x,t) \\ &u(0,y,t) = g_4(y,t), \quad u(L_x,y,t) = g_2(y,t), \quad 0 \le t \le t_f. \end{aligned} \tag{1. 2}$$

Heat conduction phenomena with suitable boundary conditions exist frequently in many areas of science and engineering, see, for example, [4, 5, 11, 12, 13, 14, 15, 10, 2]. Historically, highly accurate compact finite difference (CFD) schemes are developed by Lele [9]. However, these higher-order CFD schemes offer good accuracy only at the interior nodes or for periodic boundary conditions. The low-order of accuracy near boundary nodes affect the whole numerical results and reduces the accuracy of overall numerical solution [3].

The CFD schemes are quite efficient as compared to many other classical methods [1]. On Cartesian uniform meshes, these schemes provide a higher-order of accuracy with only a compact stencil [8]. The CFD schemes not only provide fast convergence but are also numerically stable. One of the most important property of CFD schemes is their non-oscillatory behavior. In the wave propagation phenomenon, these schemes play an important role [16].

By using Local One Dimension (LOD) method, Jennifer. Z [6] has developed fourth-order globally solvable, unconditionally stable, and convergent CFD schemes for multidimensional heat conduction equation with Neumann boundary conditions. The LOD method consists on mainly two aspects:
(I) Splitting of the differential equation;
(II) Discretization of resulting 1-D equations.

By using LOD method, the 2-D heat conduction equation is splitted into the corresponding two 1-D equations:

$$\frac{1}{2}U_t = U_{xx} + \frac{1}{2}F(x,y,t), \tag{1. 3}$$

$$\frac{1}{2}U_t = U_{yy} + \frac{1}{2}F(x,y,t). \tag{1. 4}$$

Then by using Crank-Nicholson time integrator on these equations, second-order accurate approximation for time was obtained. After that, by further treatment on spatial derivative, fourth-order approximation over the whole domain was obtained.

Here, we are oriented to construct sixth-order implicit finite difference (IFD) scheme for 2-D heat conduction problem. The most crucial point is to provide the construction of the scheme for boundary enclosure in a way that we can maintain the order of accuracy of interior node scheme as well as the stability of time integrator. Initially, a numerical scheme is constructed for 1-D heat conduction equation and then extended to 2-D by using Kronecker product.

2. Sixth-order implicit finite difference scheme

Suppose, we discretize the spatial interval $[a_x, b_x]$ in to $x_n + 2$ nodes. The grid points can be computed as

$$x_i = a_x + (i-1)h_x, \qquad \text{for } i = 1, 2, \cdots, n+2, \tag{2. 5}$$

where, $h_x = \frac{(b_x - a_x)}{n_x - 1}$. Note it that, we have x_n interior nodes and two boundary nodes. Boundary conditions are provided at nodes x_1 and x_{n+2}. We intend to construct sixth-order IFD scheme for second-order derivatives at nodes adjacent to boundary nodes, i.e., x_2, x_3, x_n, x_{n+1}, and the interior nodes x_i. Due to symmetry, we only present construction of the proposed scheme for the one-sided nodes, i.e., x_2 and x_3.

The stencil used for sixth-order IFD scheme to approximate second-order derivatives is

$$(i-2, i-1, i, i+1, i+2) \qquad \text{for } i = 3, 4, \cdots, n.$$

The stencil tells us that if we are standing at location i, then we need two mesh points left of i and two mesh points right of it.

2.1. **Generalized sixth-order implicit finite difference scheme.** Suppose, we are interested to make sixth-order finite difference approximations of second order derivatives at the interior nodes x_i. To this end, we first write a prototype for the scheme with some unknowns

$$\beta T''_{i-2} + \alpha T''_{i-1} + T''_i + \alpha T''_{i+1} + \beta T''_{i+2} = \frac{1}{h^2}(a_1 T_{i-2} - (\sum_{i=1}^{3} a_i) T_{i-1} + a_2 T_i + a_3 T_{i+1} + a_4 T_{i+2}), \tag{2. 6}$$

where α, β, a_1, a_2, a_3, and a_4 are unknowns to be determined in such a way that we can get sixth-order accurate approximations of second-order derivatives. The Taylor's expansion of equation (2. 6) around the central nodes x_i gives the following system of six linear algebraic equations in six unknowns:

$$\begin{aligned}
a4 &= 0,\\
-3/2\, a1 + a2/2 - 2\, a4 + 2\,\beta + 2\,\alpha + 1 &= 0,\\
-5/8\, a1 + a2/24 - 2/3\, a4 + 4\,\beta + \alpha &= 0,\\
\frac{31\, a1}{120} - \frac{a2}{120} - \frac{a3}{60} - \frac{4\, a4}{15} &= 0,\\
-\frac{7\, a1}{80} + \frac{a2}{720} - \frac{4\, a4}{45} + 4/3\,\beta + \alpha/12 &= 0,\\
\frac{127\, a1}{5040} - \frac{a2}{5040} - \frac{a3}{2520} - \frac{8\, a4}{315} &= 0.
\end{aligned} \tag{2. 7}$$

By solving the system given in equation (2. 7), we get the values of unknown parameters and the error term as

$$a1 = 0,\ a2 = \frac{-240}{97},\ a3 = \frac{120}{97},\ a4 = 0, \alpha = \frac{12}{97},\ \beta = \frac{-1}{194}. \tag{2. 8}$$

$$E = -\frac{31\, h^6 f_8}{48888} - \frac{11\, h^8 f_{10}}{183330} + O(h^{10}) \tag{2. 9}$$

Then equation (2. 6) becomes

$$\tfrac{-1}{194}(T''_{i-2} - 24T''_{i-1} - 194T''_{i} - 24T''_{i+1} + T''_{i+2}) = \tfrac{120}{97h^2}(0T_{i-2} + T_{i-1} - 2T_i + T_{i+1} + 0T_{i+2}). \tag{2. 10}$$

The equation (2. 10) can be written as

$$\frac{-1}{194}\begin{bmatrix}1 & -24 & -194 & -24 & 1\end{bmatrix}\begin{bmatrix}T''_{i-2}\\ T''_{i-1}\\ T''_{i}\\ T''_{i+1}\\ T''_{i+2}\end{bmatrix} = \frac{120}{97h^2}\begin{bmatrix}0 & 1 & -2 & 1 & 0\end{bmatrix}\begin{bmatrix}T_{i-2}\\ T_{i-1}\\ T_{i}\\ T_{i+1}\\ T_{i+2}\end{bmatrix}, \tag{2. 11}$$

where, $i = 3, 4, \cdots, n$. Equation (2. 11) can also be written as

$$\frac{-1}{194}\begin{bmatrix}1 & -24 & -194 & -24 & 1 & \cdots & 0 & 0 & 0\\ 0 & 1 & -24 & -194 & -24 & 1 & \cdots & 0 & 0\\ 0 & 0 & 1 & -24 & -194 & -24 & 1 & \cdots & 0\\ \vdots & \vdots & \vdots & \ddots & \ddots & \ddots & \ddots & \ddots & \vdots\\ 0 & 0 & 0 & \cdots & 1 & -24 & -194 & -24 & 1\end{bmatrix}\begin{bmatrix}T''_1\\ T''_2\\ T''_3\\ \vdots\\ T''_{n+2}\end{bmatrix}$$

$$= \frac{120}{97h^2}\begin{bmatrix}0 & 1 & -2 & 1 & 0 & \cdots & 0 & 0 & 0\\ 0 & 0 & 1 & -2 & 1 & 0 & \cdots & 0 & 0\\ 0 & 0 & 0 & 1 & -2 & 1 & 0 & \cdots & 0\\ \vdots & \vdots & \vdots & \ddots & \ddots & \ddots & \ddots & \ddots & \vdots\\ 0 & 0 & 0 & \cdots & 0 & 1 & -2 & 1 & 0\end{bmatrix}\begin{bmatrix}T_1\\ T_2\\ T3\\ \vdots\\ T_{n+2}\end{bmatrix}. \tag{2. 12}$$

2.2. **Sixth-order implicit finite difference scheme for nodes x_2 and x_{n+1}.** Consider the following relationship

$$T''_2 + \alpha T''_3 + \beta T''_4 = \tfrac{1}{h^2}(a_1T_1 - (\textstyle\sum_{i=1}^{7} a_i)T_2 + a_2T_3 + a_3T_4 + a_4T_5 + a_5T_6 + a_6T_7 + a_7T_8). \tag{2. 13}$$

By expanding equation (2. 13) around x_2, we get the following system of seven linear algebraic equations in seven unknowns:

$$
\begin{aligned}
-a2 - 2\,a3 - 3\,a4 - 4\,a5 - 5\,a6 - 6\,a7 + a1 &= 0,\\
-a1/2 - a2/2 - 2\,a3 - 9/2\,a4 - 8\,a5 - \frac{25}{2}\,a6 - 18\,a7 + \frac{217}{194} &= 0,\\
a1/6 - a2/6 - 4/3\,a3 - 9/2\,a4 - \frac{32\,a5}{3} - \frac{125\,a6}{6} - 36\,a7 + \frac{11}{97} &= 0,\\
-a1/24 - a2/24 - 2/3\,a3 - \frac{27\,a4}{8} - \frac{32\,a5}{3} - \frac{625\,a6}{24} - 54\,a7 + \frac{5}{97} &= 0,\\
\frac{a1}{120} - \frac{a2}{120} - \frac{4\,a3}{15} - \frac{81\,a4}{40} - \frac{128\,a5}{15} - \frac{625\,a6}{24} - \frac{324\,a7}{5} + \frac{4}{291} &= 0,\\
-\frac{a1}{720} - \frac{a2}{720} - \frac{4\,a3}{45} - \frac{81\,a4}{80} - \frac{256\,a5}{45} - \frac{3125\,a6}{144} - \frac{324\,a7}{5} + \frac{1}{582} &= 0,\\
\frac{a1}{5040} - \frac{a2}{5040} - \frac{8\,a3}{315} - \frac{243\,a4}{560} - \frac{1024\,a5}{315} - \frac{15625\,a6}{1008} - \frac{1944\,a7}{35} - \frac{1}{2910} &= 0.
\end{aligned}
\tag{2. 14}
$$

By solving the system given in equation (2. 14), we get the following values of unknowns and the error term as

$$
a1 = \frac{12089}{17460},\ a2 = -\frac{5757}{1940},\ a3 = \frac{4237}{873},\ a4 = -\frac{12821}{3492},\ a5 = \frac{6843}{3880},\ a6 = -\frac{8539}{17460},\ a7 = \frac{1043}{17460}. \tag{2. 15}
$$

$$
E = -\frac{2357\,h^6 f_8}{46560} - \frac{10615\,h^7 f_9}{97776} + O(h^8) \tag{2. 16}
$$

Whereas, the values of α and β are same as defined in the generalized sixth-order IFD scheme. Substituting the values of unknowns in equation (2. 13), we have

$$
\frac{1}{194}(194T_2'' + 24T_3'' - T_4'')
$$

$$
= \frac{1}{h^2}\left(\frac{12089}{17460}T_1 + \frac{558}{2315}T_2 - \frac{5757}{1940}T_3 + \frac{4237}{873}T_4 - \frac{12821}{3492}T_5 + \frac{6843}{3880}T_6 - \frac{8539}{17460}T_7 + \frac{1043}{17460}T_8\right). \tag{2. 17}
$$

Equation (2. 17) can also be written as

$$
\frac{1}{194}\begin{bmatrix}194 & 24 & -1\end{bmatrix}\begin{bmatrix}T_2'' \\ T_3'' \\ T_4''\end{bmatrix}
$$

$$= \frac{1}{h^2}\begin{bmatrix}\frac{12089}{17460} & \frac{558}{2315} & -\frac{5757}{1940} & \frac{4237}{873} & -\frac{12821}{3492} & \frac{6843}{3880} & -\frac{8539}{17460} & \frac{1043}{17460}\end{bmatrix}\begin{bmatrix}T_1\\T_2\\\vdots\\T_8\end{bmatrix}. \quad (2.\ 18)$$

Similarly, we can write the stencil for x_{n+1} as

$$\begin{bmatrix}1 & \alpha & \beta\end{bmatrix}\begin{bmatrix}T''_{(i-1)}\\T''_i\\T''_{(i+1)}\end{bmatrix}\frac{1}{h^2} = \begin{bmatrix}a_1 & -\left(\sum_{i=1}^{i=7} a_i\right) & a_2 & a_3 & a_4 & a_5 & a_6 & a_7\end{bmatrix}\begin{bmatrix}T_1\\T_2\\\vdots\\T_8\end{bmatrix}. \quad (2.\ 19)$$

2.3. **Sixth-order implicit finite difference scheme for nodes x_3 and x_n.** Consider the following relationship

$$\alpha T_2'' + T_3'' + \alpha T_4'' + \beta T_5''$$
$$= \frac{1}{h^2}(a_1T_1 + a_2T_2 - (\sum_{i=1}^{7} a_i)T_3 + a_3T_4 + a_4T_5 + a_5T_6 + a_6T_7 + a_7T_8). \quad (2.\ 20)$$

By expanding equation (2. 20) around x_3, we obtain the following system of linear algebraic equations:

$$\begin{aligned}
-4\,a6 - 5\,a7 + 2\,a1 + a2 - a3 - 2\,a4 - 3\,a5 &= 0,\\
-2\,a1 - a2/2 - a3/2 - 2\,a4 - 9/2\,a5 - 8\,a6 - \frac{25}{2}\,a7 + \frac{241}{194} &= 0,\\
4/3\,a1 + a2/6 - a3/6 - 4/3\,a4 - 9/2\,a5 - \frac{32\,a6}{3} - \frac{125\,a7}{6} - \frac{1}{97} &= 0,\\
-2/3\,a1 - a2/24 - a3/24 - 2/3\,a4 - \frac{27\,a5}{8} - \frac{32\,a6}{3} - \frac{625\,a7}{24} + \frac{11}{97} &= 0, \quad (2.\ 21)\\
\frac{4\,a1}{15} + \frac{a2}{120} - \frac{a3}{120} - \frac{4\,a4}{15} - \frac{81\,a5}{40} - \frac{128\,a6}{15} - \frac{625\,a7}{24} - \frac{2}{291} &= 0,\\
-\frac{4\,a1}{45} - \frac{a2}{720} - \frac{a3}{720} - \frac{4\,a4}{45} - \frac{81\,a5}{80} - \frac{256\,a6}{45} - \frac{3125\,a7}{144} + \frac{2}{291} &= 0,\\
\frac{8\,a1}{315} + \frac{a2}{5040} - \frac{a3}{5040} - \frac{8\,a4}{315} - \frac{243\,a5}{560} - \frac{1024\,a6}{315} - \frac{15625\,a7}{1008} - \frac{2}{1455} &= 0.
\end{aligned}$$

By solving the system given in equation (2. 21), we obtain the values of unknowns and the error term as

$$a1 = \frac{469}{17460},\ a2 = \frac{2177}{1940},\ a3 = \frac{3371}{3492},\ a4 = \frac{41}{194},\ a5 = -\frac{201}{1940},\ a6 = \frac{1019}{34920},$$
$$a7 = -\frac{7}{1940}. \quad (2.\ 22)$$

$$E = \frac{2647\,h^6 f_8}{977760} + \frac{349\,h^7 f_9}{97776} + O(h^8) \tag{2. 23}$$

As before, the values of α and β are same as defined for generalized IFD scheme. After substituting the values of unknowns in equation (2. 20), we get the following equation

$$\frac{1}{194}\left(24T_2'' + 194T_3'' + 24T_4'' - T_5''\right)$$

$$= \tfrac{1}{h^2}\left(\tfrac{469}{17460}T_1 + \tfrac{2177}{1940}T_2 + \tfrac{3149}{1401}T_3 + \tfrac{3371}{3492}T_4 + \tfrac{41}{194}T_5 - \tfrac{201}{1940}T_6 + \tfrac{1019}{34920}T_7 - \tfrac{7}{1940}T_8\right). \tag{2. 24}$$

Equation (2.3) can also be written as

$$\frac{1}{194}\begin{bmatrix}24 & 194 & 24 & -1\end{bmatrix}\begin{bmatrix}T_2''\\ T_3''\\ T_4''\\ T_5''\end{bmatrix}$$

$$= \frac{1}{h^2}\begin{bmatrix}\tfrac{469}{17460} & \tfrac{2177}{1940} & \tfrac{3149}{1401} & \tfrac{3371}{3492} & \tfrac{41}{194} & -\tfrac{201}{1940} & \tfrac{1019}{34920} & -\tfrac{7}{1940}\end{bmatrix}\begin{bmatrix}T_1\\ T_2\\ \vdots\\ T_8\end{bmatrix}. \tag{2. 25}$$

Similarly, we can write the stencil for x_n as

$$\begin{bmatrix}\alpha & 1 & \alpha & \beta\end{bmatrix}\begin{bmatrix}T_{i-2}''\\ T_{i-1}''\\ T_i''\\ T_{i+1}''\end{bmatrix} = \frac{1}{h^2}\begin{bmatrix}a_1 & a_2 & -\left(\sum_{i=1}^{i=7} a_i\right) & a_3 & a_4 & a_5 & a_6 & a_7\end{bmatrix}\begin{bmatrix}T_1\\ T_2\\ \vdots\\ T_8\end{bmatrix}. \tag{2. 26}$$

To illustrate the procedure for the conversion of the above developed 1-D schemes in to 2-D schemes, consider the following 2-D heat conduction equation

$$U_t = K_1 U_{(xx)} + K_2 U_{(yy)} + s(x,y,t), \qquad 0 \le x, y \le 1, \quad t \le t_f, \tag{2. 27}$$

where, s(x,y,t) is the source term. Assume that the analytic solution of 2-D heat equation is

$$U(x,y,t) = e^{-t^2} sin(\pi x) sin(\pi y). \tag{2. 28}$$

Differentiating equation (2. 28) twice w.r.t. x and y and taking first derivative w.r.t. t, then by subsituting these values in equation (2. 27) we have the following expression

$$s(x,y,t) = ((K_1 + K_2)\pi^2 - 2t)U. \tag{2. 29}$$

Suppose, we have a differential operator that computes second-order derivatives, i.e.,

$$U_{(xx)} = A_1 U(:,y,t),$$

$$U_{(yy)} = A_2 U(x,:,t).$$

For 2-D scheme, we construct the differential operator as

$$A = K_1(I_y \times A_1) + K_2(A_2 \times I_x). \tag{2. 30}$$

Then equation (2. 27) becomes

$$U_t(t) = AU(t) + s(t). \tag{2. 31}$$

Now we use Crank-Nicholson method to solve equation (2. 31) as follows

$$\frac{U^{(n+1)} - U^n}{\Delta t} = A\frac{U^{(n+1)} + U^n}{2} + \frac{S^{(n+1)} + S^n}{2}, \tag{2. 32}$$

$$U^{(n+1)} - U^n = \frac{\Delta t}{2}AU^{(n+1)} + \frac{\Delta t}{2}AU^n + \frac{\Delta t}{2}(S^{(n+1)} + S^n). \tag{2. 33}$$

Let

$$S^{(n+1/2)} = \frac{S^{(n+1)} + S^n}{2}, \qquad r = \frac{\Delta t}{2}.$$

Then, we have

$$U^{(n+1)} - U^n = rAU^{(n+1)} + rAU^n + \Delta t s^{(n+1/2)}, \tag{2. 34}$$

$$(I - rA)U^{(n+1)} = (I + rA)U^n + \Delta t S^{(n+1/2)}. \tag{2. 35}$$

Equation (2. 35) can be simplified as follows

$$U^{(n+1)} = B_1^{-1}(B_2 U^n + \Delta t s^{n+1/2}), \tag{2. 36}$$

where,

$$B_1 = I - rA,$$
$$B_2 = I + rA,$$
$$I = \text{identity matrix}$$

This is how we convert one-dimensional IFD schemes in to two-dimensional IFD schemes.

3. Stability

After spatial discretization of 1-D heat conduction equation, we get

$$\begin{aligned} \mathbf{T}_t(t) &= k\mathbf{T}_{xx}(t) + \mathbf{S}(t) \\ \mathbf{T}_t(t) &= \frac{k}{h^2}\mathbf{A}^{-1}\mathbf{B}\mathbf{T}(t) + \mathbf{S}(t)\,, \end{aligned} \tag{3. 37}$$

where, $\mathbf{A}\mathbf{T}_{xx} = \frac{1}{h^2}\mathbf{B}\mathbf{T}$. We apply Crank-Nicolson method on the above equations for temporal discretization and get

$$\begin{aligned} \frac{\mathbf{T}(t_{i+1}) - \mathbf{T}(t_i)}{\Delta t} &= \frac{k}{h^2}\mathbf{A}^{-1}\mathbf{B}\left(\frac{\mathbf{T}(t_{i+1}) - \mathbf{T}(t_i)}{2}\right) + \frac{\mathbf{S}(t_{i+1}) + \mathbf{S}(t_i)}{2} \\ \mathbf{T}(t_{i+1}) &= \left(\mathbf{I} - r\mathbf{A}^{-1}\mathbf{B}\right)^{-1}\left(\mathbf{I} + r\mathbf{A}^{-1}\mathbf{B}\right)\mathbf{T}(t_i) + \left(\mathbf{I} - r\mathbf{A}^{-1}\mathbf{B}\right)^{-1}\Delta t\mathbf{S}^{i+1/2}\,, \end{aligned} \tag{3. 38}$$

where $r = \frac{k\Delta t}{2h^2}$ and $\mathbf{S}^{i+1/2} = \frac{\mathbf{S}(t_{i+1})+\mathbf{S}(t_i)}{2}$.

Now if the real parts of eigenvalues of $\left(\mathbf{I} - r\mathbf{A}^{-1}\mathbf{B}\right)^{-1}\left(\mathbf{I} + r\mathbf{A}^{-1}\mathbf{B}\right)$ are negative then the numerical scheme is stable.

One can check that λ is the eigenvalue of $\mathbf{A}^{-1}\mathbf{B}$ iff $(1 + r\lambda)/(1 - r\lambda)$ is the eigenvalue of

$\left(\mathbf{I} - r\mathbf{A}^{-1}\mathbf{B}\right)^{-1}\left(\mathbf{I} + r\mathbf{A}^{-1}\mathbf{B}\right)$. Next we will show that if $|(1+r\lambda)/(1-r\lambda)| < 1$ then real part of λ is negative.

$$\begin{aligned} \text{Take } & \left|\frac{1+r\lambda}{1-r\lambda}\right| < 1 \\ & |1+r\lambda| < |1-r\lambda| \\ & (1+r\lambda_1)^2 + r^2\lambda_2^2 < (1-r\lambda_1)^2 + r^2\lambda_2^2 \\ & 1 + r\lambda_1 < 1 - r\lambda_1 \\ & \lambda_1 < 0\,, \end{aligned} \tag{3. 39}$$

where $\lambda = \lambda_1 + i\,\lambda_2$.
For simplicity, assume the boundary conditions at nodes x_1 and x_{n+2} are zero. By including the stencils for boundaries, the approximation of second order derivative can be written as

$$\mathbf{A}\mathbf{T}_{xx} = \frac{1}{h^2}\mathbf{B}\mathbf{T}\,,$$

where $\mathbf{A}$ and $\mathbf{B}$ for $n = 10$ are

$$\mathbf{A} = \begin{bmatrix} 1 & 12/97 & -1/194 & 0 & 0 & 0 & 0 & 0 & 0 & 0 \\ 12/97 & 1 & 12/97 & -1/194 & 0 & 0 & 0 & 0 & 0 & 0 \\ -1/194 & 12/97 & 1 & 12/97 & -1/194 & 0 & 0 & 0 & 0 & 0 \\ 0 & -1/194 & 12/97 & 1 & 12/97 & -1/194 & 0 & 0 & 0 & 0 \\ 0 & 0 & -1/194 & 12/97 & 1 & 12/97 & -1/194 & 0 & 0 & 0 \\ 0 & 0 & 0 & -1/194 & 12/97 & 1 & 12/97 & -1/194 & 0 & 0 \\ 0 & 0 & 0 & 0 & -1/194 & 12/97 & 1 & 12/97 & -1/194 & 0 \\ 0 & 0 & 0 & 0 & 0 & -1/194 & 12/97 & 1 & 12/97 & -1/194 \\ 0 & 0 & 0 & 0 & 0 & 0 & -1/194 & 12/97 & 1 & 12/97 \\ 0 & 0 & 0 & 0 & 0 & 0 & 0 & -1/194 & 12/97 & 1 \end{bmatrix},$$

$$\mathbf{B} = \begin{bmatrix} \frac{-8417}{34920} & \frac{-5757}{1940} & \frac{4237}{873} & \frac{-12821}{3492} & \frac{6843}{3880} & \frac{-8539}{17460} & \frac{1043}{17460} & 0 & 0 & 0 \\ \frac{2177}{1940} & \frac{-8721}{3880} & \frac{3371}{3492} & \frac{41}{194} & \frac{-201}{1940} & \frac{1019}{34920} & \frac{-7}{1940} & 0 & 0 & 0 \\ 0 & \frac{120}{97} & \frac{-240}{97} & \frac{120}{97} & 0 & 0 & 0 & 0 & 0 & 0 \\ 0 & 0 & \frac{120}{97} & \frac{-240}{97} & \frac{120}{97} & 0 & 0 & 0 & 0 & 0 \\ 0 & 0 & 0 & \frac{120}{97} & \frac{-240}{97} & \frac{120}{97} & 0 & 0 & 0 & 0 \\ 0 & 0 & 0 & 0 & \frac{120}{97} & \frac{-240}{97} & \frac{120}{97} & 0 & 0 & 0 \\ 0 & 0 & 0 & 0 & 0 & \frac{120}{97} & \frac{-240}{97} & \frac{120}{97} & 0 & 0 \\ 0 & 0 & 0 & 0 & 0 & 0 & \frac{120}{97} & \frac{-240}{97} & \frac{120}{97} & 0 \\ 0 & 0 & 0 & \frac{-7}{1940} & \frac{1019}{34920} & \frac{-201}{1940} & \frac{41}{194} & \frac{3371}{3492} & \frac{-8721}{3880} & \frac{2177}{1940} \\ 0 & 0 & 0 & \frac{1043}{17460} & \frac{-8539}{17460} & \frac{6843}{3880} & \frac{-12821}{3492} & \frac{4237}{873} & \frac{-5757}{1940} & \frac{-8417}{34920} \end{bmatrix}.$$

Notice that the matrix A is a Toeplitz matrix and also strictly diagonally dominant. The matrix B is not Toeplitz due to inclusion of boundary stencils. If we neglect the first two and last two rows and columns then the remaining matrix is a Toeplitz matrix. This fact tells us as we increase the grid size, the eigenvalues of growing matrices are not random but follows a pattern or profile. In Figure 1, we have plotted the real part of eigenvalues of $A^{-1}B$ for $n = 1000$ and it shows that graph is below zeros. In other words, the real parts of all eigenvalues are negative.

By sampling eigenvalues from smaller matrices, we can tell the eigenvalues of much larger matrices by using extrapolate algorithm. Hence, it is easy to check the sign of eigenvalues in the asymptotic cases when size of the matrix is much larger. In the extrapolate

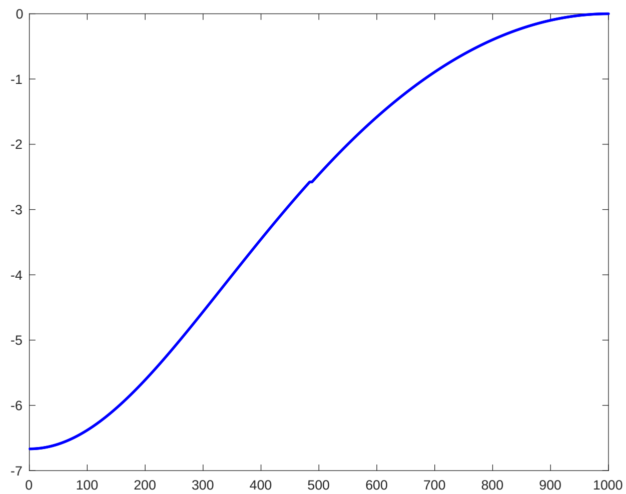

FIGURE 1. Real parts of eigenvalues of $\mathbf{A}^{-1}\mathbf{B}$ for $n = 1000$.

algorithm, the eigenvalues of sequence of banded Toeplitz matrices are not random but follow a regular pattern. This means in limit the behavior of eigenvalues of larger matrices is predictable.
In Figure 2, we have plotted the eigenvalues of $A^{-1}B \otimes I + I \otimes A^{-1}B$. Where we can see, as we increase the size of matrices their respective real part spectrum becomes closer and closer.
It means the eigenvalues are not randomly distributed but follow a regular patter. Clearly all the real parts of eigenvalues are negative. This conclude that our proposed iterative scheme is stable.

4. MULTI-DIMENSIONAL LINEAR HEAT EQUATION

It is possible to use 1-D IFD for any dimension linear heat equation on regular and rectangular grid by using Kronecker product. The IFD scheme is not valid for irregular grids in any dimension.

Consider a three dimensional linear heat equation of the form

$$U_t = K_1\, U_{xx} + K_2\, U_{yy} + K_3\, U_{zz} + s(x, y, z, t)\,.$$

Let A_x, A_y and A_z are 1-D IFD operators to approximate second order derivatives U_{xx}, U_{yy} and U_{zz} respectively. By using Kronecker product we can discretize

$$K_1\, U_{xx} + K_2\, U_{yy} + K_3\, U_{zz}$$

with the following linear operator

$$K_1\, A_x \otimes I_y \otimes I_z + K_2\, I_x \otimes A_y \otimes I_z + K_3\, I_x \otimes I_y \otimes A_z\,.$$

Generalization is straightforward for other higher dimensional cases.

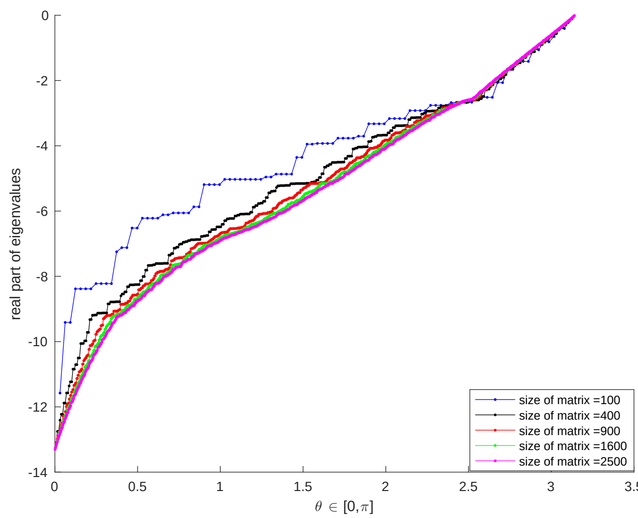

FIGURE 2. Real parts of eigenvalues of $\mathbf{A}^{-1}\mathbf{B}$ for $n = 1000$.

5. NUMERICAL TESTING

To verify numerically the order of accuracy sixth-order IFD we take the following one-dimensional problem

$$T_t(x,t) = k\,T_{xx}(x,t) \quad 0 < x < 1\,, \quad t > 0\,. \tag{5. 40}$$

This heat equation has analytical solution $T(x,t) = e^{-k\,\pi^2\,t}\,\sin(\pi\,x)$. Table 1 shows the order of accuracy for different values of k. Our numerical testing proves that IFD has at least six order of accuracy. We use

$$\text{Order of accuracy} = \log_2\left(\frac{\text{Absolute error at } h}{\text{Absolute error at } h/2}\right)$$

to compute the order of accuracy.

TABLE 1. Order of accuracy of IFD in 1-D case.

k	Δt	h	Absolute error	Order of accuracy
1	$1e-6$	0.090909	$1.5176e-6$	-
		0.047619	$6.1566e-9$	7.9455
$1e-3$	$1e-6$	0.090909	$2.1141e-7$	-
		0.047619	$2.3616e-9$	6.4841
$1e-5$	$1e-5$	0.090909	$2.1245e-9$	-
		0.047619	$2.9554e-11$	6.1676
$1e-7$	$1e-3$	0.090909	$2.1233e-11$	-
		0.047619	$2.8086e-13$	6.2403

To check the validity and accuracy of our developed sixth-order IFD scheme, we also solve the following 2-D example with Dirichlet boundary conditions.

$$\text{Dirichlet problem} = \begin{cases} T_t(x,y,t) = T_{xx}(x,y,t) + T_{yy}(x,y,t)\,, & 0 < x < 1,\ 0 < y < 1,\ t > 0\,, \\ T(x,y,0) = sin(\pi\,x)sin(\pi\,y)\,, & 0 \le x \le 1,\ 0 \le y \le 1\,, \\ T(x,0,t) = T(x,1,t) = 0\,, & t > 0\,, \\ T(0,y,t) = T(1,y,t) = 0\,. & \end{cases} \tag{5. 41}$$

The analytical solution to the problem (5. 41) is given in equation (5. 42).

$$T(x,y,t) = e^{-\pi^2\,t}\,sin(\pi\,x)\,sin(\pi\,y) \tag{5. 42}$$

To check the order of accuracy of IFD scheme for 2-D problem (5. 41) we took $h_1 = h_2 = h$ and $\Delta t = 1e-5$. Order of accuracy is computed in Table 2 and it ensures our theoretically proposed order of accuracy.

TABLE 2. Order of accuracy of IFD in 2-D case.

h	Absolute error	Order of accuracy
0.125	$3.9358e-06$	-
0.0666667	$1.7561e-08$	7.8081
0.0322581	$1.1598e-10$	7.2424

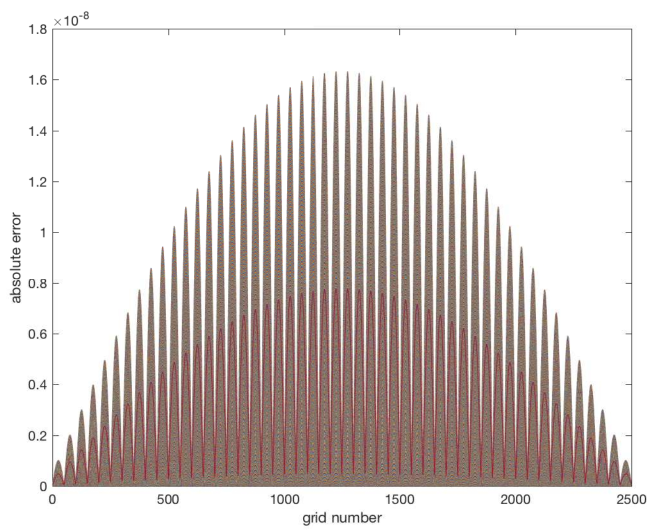

FIGURE 3. Absolute error plot.

We have performed extensive numerical testing to observe the quality of the developed sixth-order compact implicit finite difference scheme by calculating absolute error against

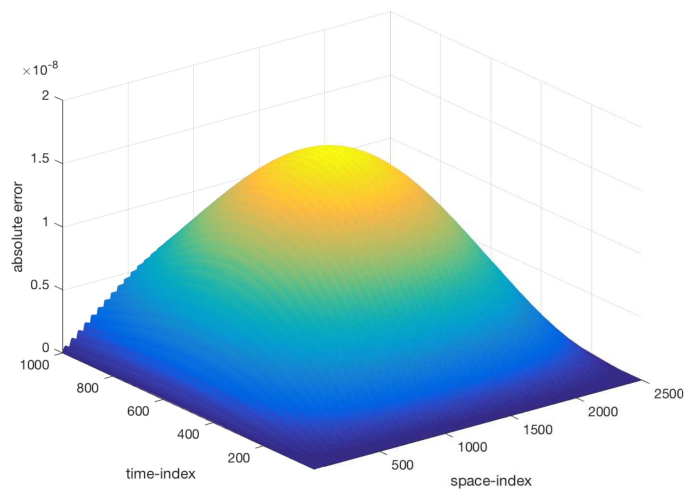

FIGURE 4. Absolute error plot.

the temporal and spatial dimensions. On top of that we also have performed numerical experiments to observe absolute error for different times.

In Figure 3, the absolute error behavior has been observed against the grid points. The maximum of the absolute error is no more than 1.62×10^{-8}. Whereas, Figure 4 combines the absolute error effect against the space index and time index.

In Figure 5, the solution sets with respect to four different time steps are plotted. While in Figure 6, absolute error has been plotted against four different time steps. When time is zero, there is no absolute error but when time gradually increases, absolute error also increases. It is shown that, for non-zero time, the maximum absolute error is ranging from approximately 1.82×10^{-10} to 1.89×10^{-9}.

In Figure 7, the solution sets have been plotted for ten different time steps. While Figure 8 beautifully explains the absolute error behaviour against ten different time steps. It has been observed that the maximum absolute error for ten different time steps is in-between approximately 3.4×10^{-11} to 1.85×10^{-9}. It has also been analyzed that the value of absolute error in the third time step is slightly increased, whereas in the remaining time steps it is increased by approximately one order of magnitude until it attains the maximum absolute error of approximately 1.85×10^{-9}.

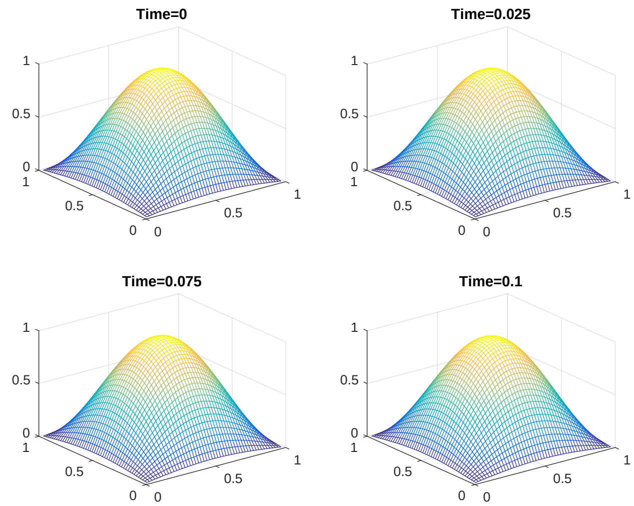

FIGURE 5. Solution plots for four different times.

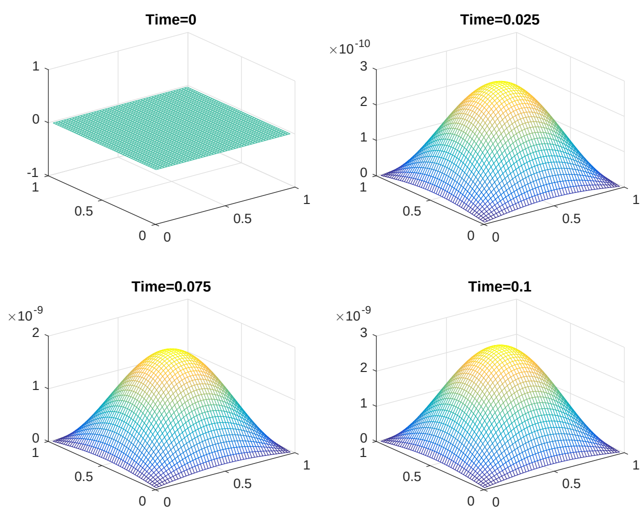

FIGURE 6. Absolute error plots for four different times.

6. CONCLUSIONS

The implicit finite difference schemes provide more accurate way to approximate the spatial derivatives as compared to explicit finite difference schemes. We have constructed

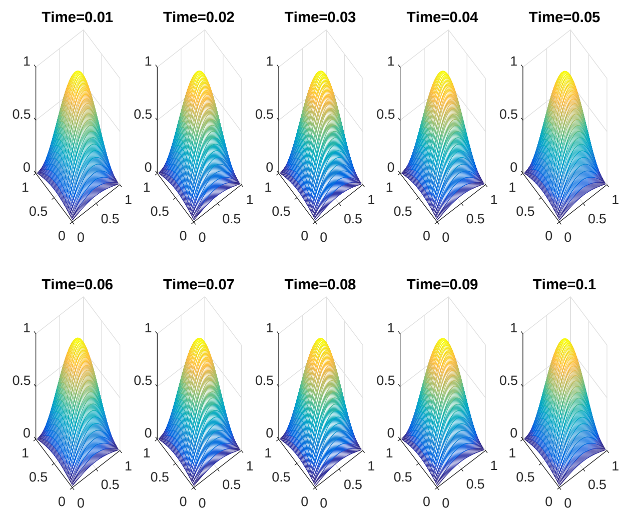

FIGURE 7. Solution plots for ten different times.

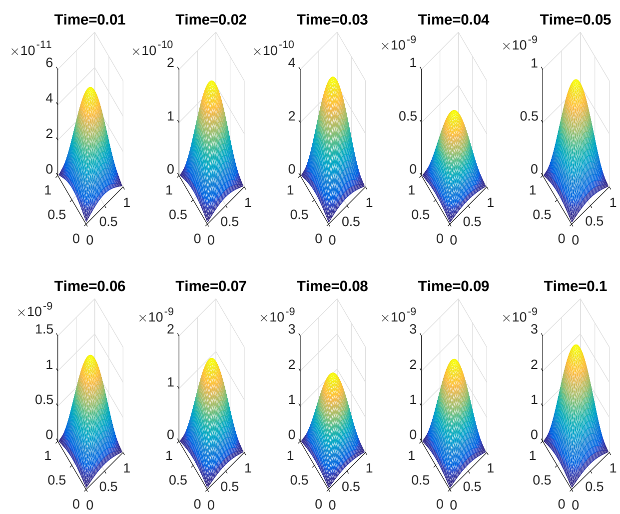

FIGURE 8. Absolute error plots for ten different times.

sixth-order implicit finite difference scheme for 1-D heat conduction problem on uniform grid, in-particular, for boundary enclosure to guarantee high order of accuracy and stability of time integrator. With the help of Kronecker product, one can extend IFD to higher dimensional heat equation on regular rectangular girds. The IFD scheme is only valid for

Dirichlet boundary conditions on regular rectangular girds. To construct higher order implicit finite different scheme with order greater than four for Neumann boundary conditions are challenging. The validity of our developed numerical scheme is clearly reflected by the solved numerical example. It has been observed that the computed generalized eigenvalues of compact finite difference matrices have negative real parts that guarantees stability in the case of Crank-Nicolson method. Further work can be done by developing such schemes for more complicated problems; see, for example, [7].

REFERENCES

[1] J. Andrew, *Finite difference weighted essentially non-oscillatory schemes with constrained transport for ideal magnetohydrodynamics*, Computational Physics (2014) 302-325.

[2] B. J. Boersma, *On the development of a 6th order accurate compact finite difference scheme for incompressible flow*, Springer, Dordrecht (2011).

[3] W. Dai, *A new accurate finite difference scheme for Neumann (insulated) boundary condition of heat conduction*, Int. J. Therm. Sci. **49**,(2010) 571. (479).

[4] W. Dai, F. Zhu and D. Y. Tzou, *A stable finite difference scheme for thermalTo investigate compact finite difference schems analysis in an N-carrier system*, Int. J. Therm. Sci. **48**,(2009) 1530-1541.

[5] A. Faghri and Y. Zhang, *Transport Phenomena in Multiphase Systems*, Elsevier, UK, (2006) 1530-1541.

[6] Z. Jennifer, *Fourth-order compact schemes for solving multidimensional heat problems with Neumann boundary conditions*, Numerical Methods for Partial Differential Equations (2008) 165-178.

[7] H. Khalil, R. A. Khan, M. H. Al-Smadi and A. A. Freihat, *Approximation of Solution of Time Fractional Order Three-Dimensional Heat Conduction Problems with Jacobi Polynomials* , Punjab Univ. j. math. **47**, No. 1 (2015) 35-56.

[8] C. Lacor, *A finite volume formulation for compact schemes on arbitrary meshes with applications to LES*, Computational Fluid Dynamics (2001) 479-484.

[9] S. K. Lele, *Compact finite difference schemes with spectral-like resolution*, J. Comput. Phys. **103**,(1992) 16-42.

[10] W. Lia, *On the dispersion, stability and accuracy of a compact higher-order finite difference scheme for 3D acoustic wave equation*, Computational and Applied Mathematics (2014) 571-583.

[11] T. Q. Qiu and C. L. Tien, *Short-pulse laser heating on metals*, Int. J. Heat Mass Transfer **35**,(1992) 719-726.

[12] T. Q. Qiu and C. L. Tien, *Heat transfer mechanisms during short-pulse laser heating of metals*, ASME J. Heat Transfer **115**,(1993).

[13] D. Y. Tzou, *A unified field approach for heat conduction from micro to macro-scales*, ASME J. Heat Transfer **117**,(1995) 8-16.

[14] D. Y. Tzou, *Macro to Microscale Heat Transfer: the Lagging Behavior*, Taylor & Francis, Washington D.C., (1997).

[15] D.Y. Tzou and W. Dai, *Thermal lagging in multi-carrier systems*, Int. J. Heat Mass Transfer **52**,(2009) 1206-1213.

[16] H. Zhou, *Prefactored optimized compact finite-difference schemes for second spatial derivatives*, GEOPHYSICS (2011) WB87-WB95.